JME

Journal of Mining & Environment,
Vol. 9, No. 3, 2018, 547-557.
DOI: 10.22044/jme.2018.5960.1410

Computational fluid dynamics simulations for investigation of parameters affecting goaf gas distribution

K.M. Tanguturi* and R.S. Balusu

Energy Flagship, CSIRO, Pullenvale, Kenmore, Australia

Received 3 July 2017; received in revised form 1 February 2018; accepted 13 February 2018
**Corresponding author: krishna.tanguturi@csiro.au (K.M. Tanguturi).*

Abstract

It is necessary to obtain a fundamental understanding of the goaf gas flow patterns in longwall mine in order to develop optimum goaf gas drainage and spontaneous combustion (sponcom) management strategies. The best ventilation layout for a longwall underground mine should assist in goaf gas drainage and further reduce the risk of sponcom in the goaf. Further, in the longwall panel, regulators are installed in the maingate (MG) seals to control the gas migration on the MG side and the mine operators frequently encountered with seals leakage problems leading to abnormal gas contents in the tube bundles. Extensive parametric studies were carried out to investigate the effects of ventilation layouts, regulators, and seals leakages on the goaf gas distribution using the Computational Fluid Dynamics (CFD) techniques. The results of various CFD simulations are presented and discussed in detail in this paper.

Keywords: *CFD, Ventilation Layout, Goaf, Rear Shaft, Seals, Regulators.*

1. Introduction

In high gassy mining conditions and in coal seams prone to spontaneous combustion (sponcom), management of safety and economics issues is critical for a successful operation of longwall, particularly in longer panels [1, 2]. CSIRO has been engaged in the investigation of gas flow migration dynamics within longwall goaf areas with the objective of improving gas capture, minimizing the risk of spontaneous combustion, and developing effective goaf inertization strategies. A major component of this work is the development of CFD models to simulate the various scenarios of ventilation arrangements, and understand the gas distribution due to seals leakages and from installation of regulators in the MG side cut-through. This approach not only helps the design of innovative gas management strategies but also the control of spontaneous combustion risk in the goaf.

CFD modelling has been used in the coal mining industry in a number of areas by various researchers. Two-dimensional CFD models based on the theory of natural convection and heat transfer in porous media were used to study the flow and temperature fields in underground coal fires [3]. CFD studies were conducted by National Institute for Occupational Safety and Health (NIOSH) and Mine Safety and Health Administration (MSHA) to investigate the temperature characteristics of mine fire [4]. Coal dust explosions are one of the most significant hazards in underground mines. A series of comprehensive studies were conducted [5, 6] using CFD simulations to model coal dust explosions and the effectiveness of active explosion barriers. Longwall dust control near the shearer region using dust capturing scrubber was investigated numerically and experimentally [7]. CFD models were used to investigate the high methane-level problems on the tail gate side of the goaf and the various control options [8]. A fundamental investigation of the goaf gas displacement due to the buoyancy effects from the longwall panel orientations was carried out numerically [9]. Various other investigations were carried out using CFD techniques including simulating auxiliary ventilation layouts in rapid heading development [10], mine fires and explosions [11], control of methane and spontaneous heating [12], spontaneous combustion and heating in longwall [13, 14], and in other applications in mineral processing [15]. This paper presents and discusses the CFD results of various ventilation layouts, and investigates the effects of regulators and seal leakages on the goaf gas distribution.

2. CFD model

A three-dimensional CFD model of the panel was developed to obtain a fundamental understanding of the goaf gas flow patterns in a 1.0 km long goaf. The working seam thickness was 3.6 m, which represented the face height. The longwall panel width was 300 m and the roadway width on both the MG and tailgate (TG) sides of the face was 5.4 m. The goaf height up to 80 m above the working seam and the floor strata down to 12 m below the working seam was included in the CFD model. In the model, MG and TG cut-throughs were spaced at every 100 m interval along the length of the goaf, and were 75 m long and 5 m wide. The rear shaft was of 2.1 m diameter located at the start-up areas of the panel in the CFD model. The total elevation difference from the start-up area to the face was about 36 m in the 1.0 km long CFD model. It is to be noted that the face was at 36 m higher elevation compared to the face start-up area in the 1.0 km model, whereas in the 500 m start-up area model, the elevation difference was around 22 m.

3. Mathematical models

The instantaneous flow conservative equations, i.e. the continuity, momentum, and species transport equations were solved numerically using the finite volume discretization techniques. These equations were solved in the laminar flow goaf region. In the CFD model, the incorporation of goaf spatial permeability distribution and gas emission rates was via the user defined function (UDF), which was linked to the solver.

3.1. Instantaneous equations

Continuity equation:

$$\nabla \bullet \vec{V} = 0.0 \tag{1}$$

Steady State Navier Stokes Equation:

$$(\vec{V} \bullet \nabla)\rho \vec{V} = -\nabla p + \mu \nabla^2 \vec{V} + \rho \vec{f} \tag{2}$$

Steady State Species Transport Equation:

$$(\vec{V_s} \bullet \nabla)\rho Y_s = D_{ms} \nabla^2 Y + \dot{\omega}_s \tag{3}$$

where subscript *s* represents the specific generation of the species O_2, CH_4, and N_2.

In the goaf region, the momentum drop per unit volume was modelled via a Used Defined Function (UDF), in which the spatial permeability of the goaf in three directions was specified and the specific momentum drop was calculated. The permeability distribution in the goaf area varied considerably at different locations based on the goaf fall, and it ranged from 10^3 millidarcy (md) to 10^{10} md in the goaf area, and went up to 10^{12} md in the collapsed roadways just behind the face.

3.2. Time-averaged governing equations

In the face region, the flow was treated as turbulent, and the time/Reynolds averaged equations were solved. The two-equation standard k-epsilon model [17] was used to determine the eddy viscosity and the Reynolds stress tensor. The porous media model in Ansys Fluent [16] was used to simulate the flow in the face where the momentum drop per unit volume in the leg and the other linkages in the shield were introduced in the source term to the standard turbulent fluid flow equations. The source term was composed of two parts: a viscous loss term (Darcy law) and an inertial loss term (as given in Equation 7).

Time-Averaged Continuity Equation:

$$\nabla \bullet \overline{\vec{V}} = 0.0 \tag{4}$$

Reynolds-Averaged Navier-Stokes Equation:

$$(\overline{\vec{V}} \bullet \nabla)\rho \overline{\vec{V}} = -\nabla \overline{P} + \mu \nabla^2 \overline{\vec{V}} + \vec{S} + \nabla : \tau_R \tag{5}$$

$$\vec{S} = -\left(\sum_{j=1}^{3} D_{ij} \mu \overline{\vec{V}} + \sum_{j=1}^{3} C_{ij} \frac{1}{2} \rho \left| \overline{\vec{V}} \right| \overline{\vec{V}} \right) \tag{6}$$

where τ_R is the Reynolds stress tensor, which represents the additional stresses induced in the flow due to turbulence.

Turbulent Kinetic Energy-k Equation:

$$\rho \overline{u}_j \frac{\partial k}{\partial x_j} = \tau_{ij} \frac{\partial \overline{u}_i}{\partial x_j} + \frac{\partial}{\partial x_j}\left((\mu + \frac{\mu_T}{\sigma_k}) \frac{\partial k}{\partial x_j} \right) - \rho\varepsilon \tag{7}$$

where subscript *j* represents Einstein summation notation.

Turbulent Dissipation-ε Equation:

$$\rho \overline{u}_j \frac{\partial \varepsilon}{\partial x_j} = C_{\mu 1} \tau_{ij} \frac{\partial \overline{u}_i}{\partial x_j} + \frac{\partial}{\partial x_j}\left((\mu + \frac{\mu_T}{\sigma_\varepsilon}) \frac{\partial \varepsilon}{\partial x_j} \right) - C_{\mu 2} \rho \frac{\varepsilon}{k^2} \tag{8}$$

where $C_{\mu 1}$ and $C_{\mu 2}$ are the closure coefficients.

Reynolds Stress:

$$\tau_{ij} = \mu_T \left(\frac{\partial \overline{u_i}}{\partial x_j} + \frac{\partial \overline{u_j}}{\partial x_i} \right) - \frac{2}{3} \rho k \delta_{ij} \tag{9}$$

where μ_T is the eddy viscosity and δ_{ij} is the Kronecker delta.

Eddy Viscosity:

$$\mu_T = c_\mu \rho \frac{k^2}{\varepsilon} \tag{10}$$

where c_μ is the closure coefficient, which is equal to 0.07.

Second-order schemes were used to discretize the governing equations [18], and the coupling between the pressure and velocity was done using the SIMPLE algorithm [19]. All the governing equations were solved until the convergence criteria of order 10^{-5} were reached.

4. Boundary conditions

The velocity inlet boundary conditions were specified at the MG intake roadways and at the rear shaft inlet, as shown in Figure 1. From the rear intake shaft, the ventilation quantity of 30 m^3/s flew towards the MG side roadways, and an additional 30 m^3/s was drawn from the MG intake, leading to 60 m^3/s of ventilation quantity flowing across the working face.

At the TG return, the outflow boundary condition was specified. One of the other ventilation options investigated in parametric studies was using the rear shaft as a return to provide additional goaf gas management capacity in the start-up areas of the longwall panels. The longwall ventilation layout with rear shaft as return is shown in Figure 2. The airflow quantity in rear shaft as return system could be specified either through fixed exhaust fan capacity at rear shaft or through installation of a regulator in MG at inbye location of the longwall face. In the parametric simulation, the velocity inlet boundary conditions were specified at the MG intake roadways and at the rear shaft exhaust such that the total ventilation quantity of 60 m^3/s flew across the longwall face.

Another ventilation option investigated in the parametric studies was the Z ventilation system to provide additional goaf gas management capacity in case of very high goaf gas emissions in a 6 km long panel. The Z ventilation layout for longwall panel is shown in Figure 3. The airflow quantity at the rear shaft was specified through fixed exhaust fan capacity at the rear shaft. In the parametric simulation, velocity boundary conditions were specified at the MG intake roadways and at one of the TG roadways such that the total ventilation quantity of 60 m3/s flew across the longwall face.

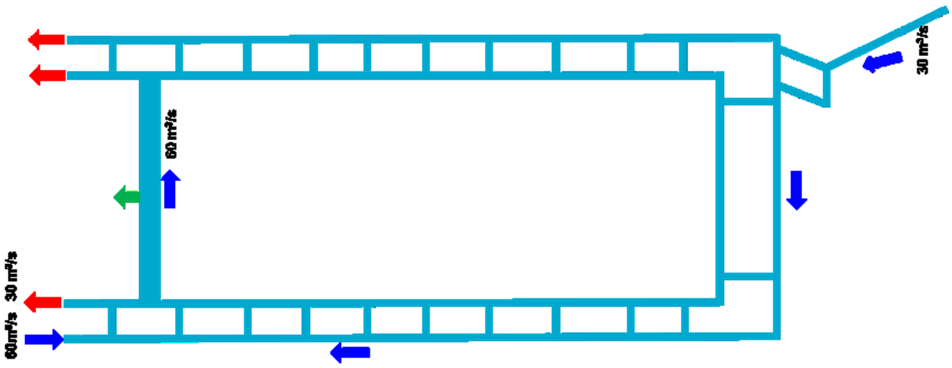

Figure 1. Longwall ventilation layout- rear shaft as intake, as used in most models.

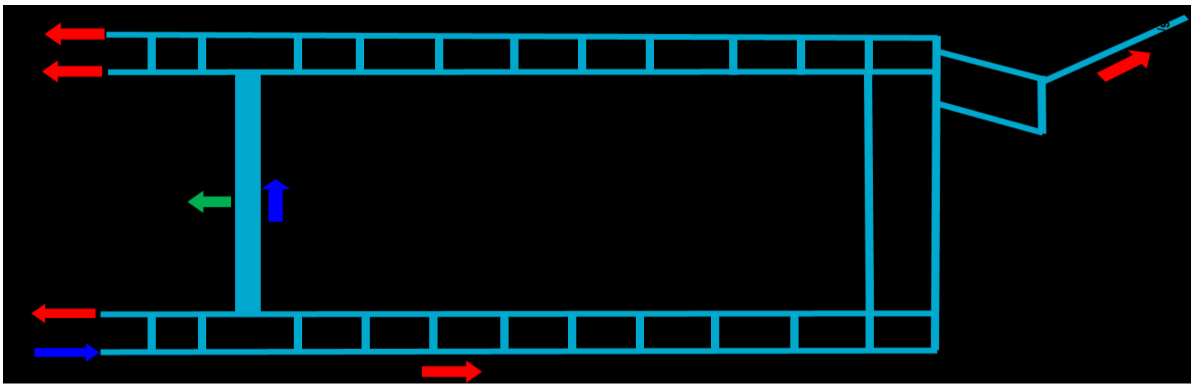

Figure 2. Longwall ventilation layout- rear shaft as return, used in parametric studies.

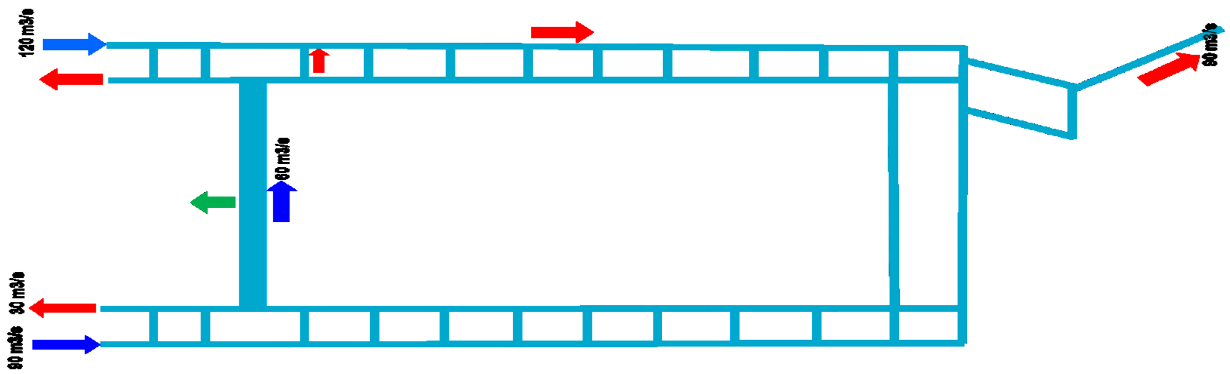

Figure 3. Longwall ventilation layout- Z ventilation, used in parametric studies.

5. Results and discussion

5.1. Gas flow modelling and validation of results

The CFD results were compared with the measured data for the validation purpose. Figure 4 shows the comparison of field data and simulated velocities at the mid-face and at 5 m from the TG corner. Figure 4 (a) shows the field data measured at various locations across the mid of the face using an anemometer, which was in concurrent with the simulated results.

The methane goaf gas emission rate was specified as 1,000 l/s in all base-case simulations for reference. The numerical results were compared with the field data for validation, as shown in Figure 5. In all the results, the gas distribution in the longwall goaf was in a plane 2 m above the seam floor. High oxygen levels at the start-up area of the panel could be attributed to the high goaf permeability, steep down dip of the panel, and from rear intake. Analysis of the results obtained show that the intake airflow seems to have a major influence on the seam level gas distribution up to 250 m behind the face, and beyond that, gas buoyancy seems to play a major role on the goaf gas distribution. The simulated results were compared with the field data obtained from tube bundle readings at various locations of the MG side of the longwall goaf. On comparison, it could be concluded that the CFD modelling results generated sensible results, and that the model could be used for various other parametric studies.

The methane gas distribution in 1.0 km long goaf of the longwall panel with rear shaft as intake is presented in Figure 6. The results obtained indicated that in the start-up area, the methane gas distribution would be symmetrical and widely distributed across the goaf area, with the highest concentration in the middle of the goaf due to flat seam gradients. This methane gas distribution profile indicates significant challenges for goaf gas drainage and suggests that there is a need for supplementary goaf gas drainage holes at the start-up area or on the MG side of the goaf, in addition to the standard TG side goaf holes.

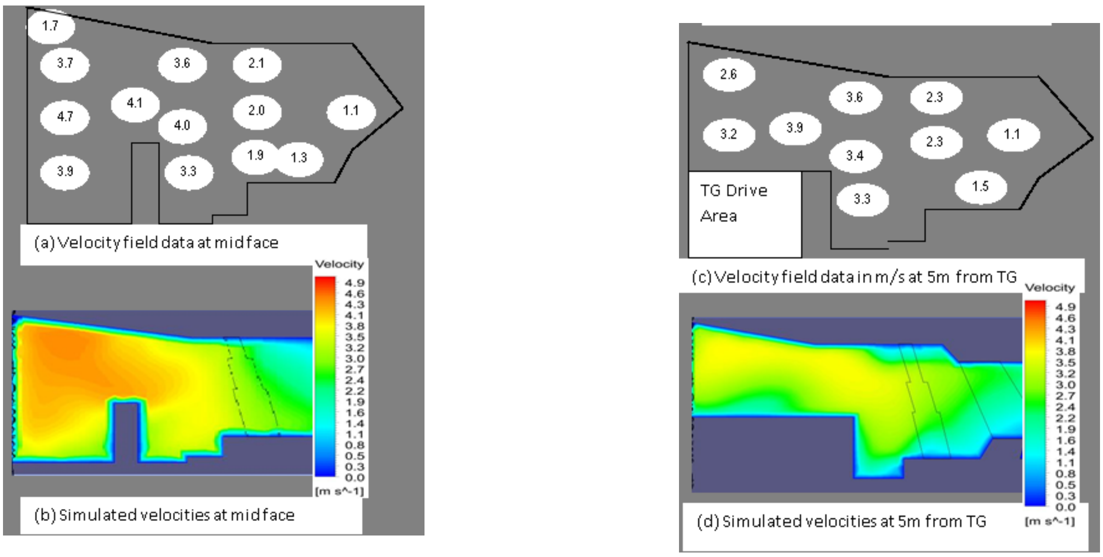

Figure 4. Comparison of measured and simulated velocities at various locations across the face.

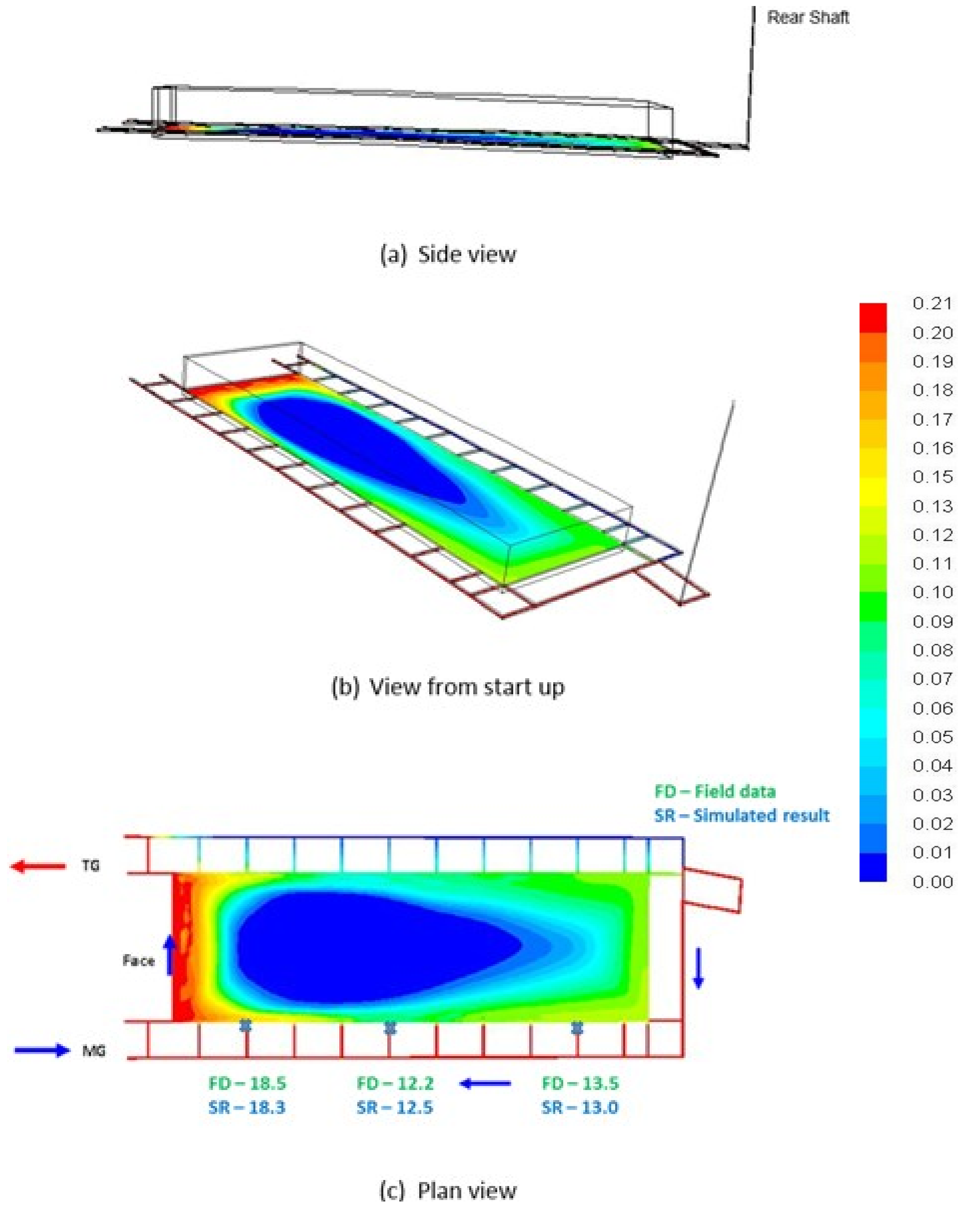

Figure 5. Oxygen distribution in the goaf–1.0 km model.

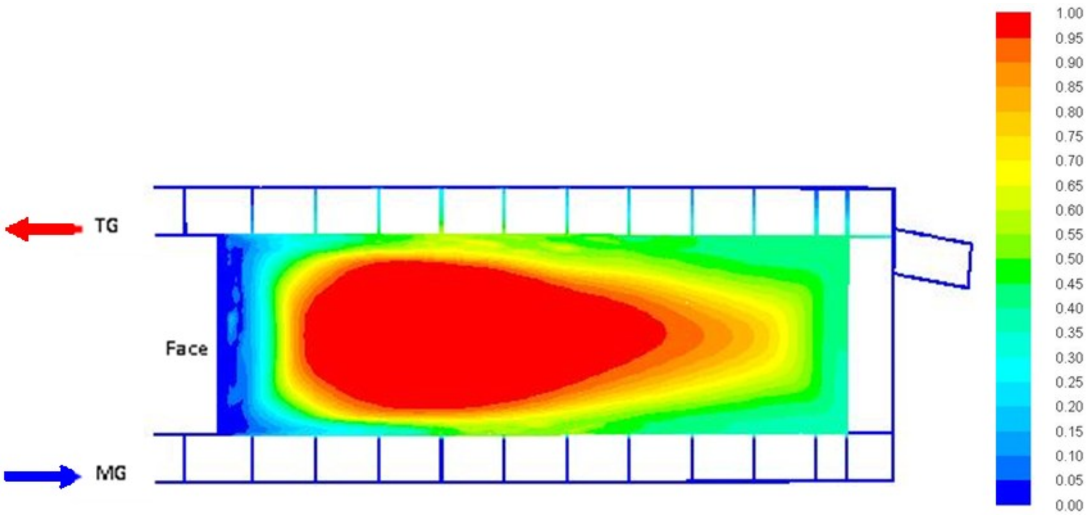

Figure 6. Methane distribution in the goaf–1.0 km model.

5.2. Mine ventilation layouts

The mine management was planned to use the rear shaft as intake to supply cool air directly to the face area in the longwall panels. In addition, it was also considered that maintenance of perimeter roadway from the rear shaft to the longwall face as intake airway was easy compared to the maintenance issues associated with perimeter roadway as the return airway. It is to be noted that in some of the Australian mines, rear shafts are used for returning the ventilation quantity [21]. Parametric studies were carried out to investigate the effects of these various ventilation layouts on the goaf gas distribution. The results obtained show that the oxygen and methane gas distributions in the goaf with three different ventilation layouts are as shown in Figures 7 and 8, respectively.

The results obtained showed that although oxygen ingress distance was significantly higher in the case of return rear shaft (Figure 7 (b)), the oxygen concentration levels on the tailgate side of the panel and at the start-up area of the panel were significantly lower, when compared with the intake rear shaft ventilation system. The results also showed that when the rear shaft was used as intake, the oxygen concentration levels at the start-up area of the panel were high at around 8-10% (Figure 7 (a)) when compared with oxygen levels of around 5–6% in the case of return rear shaft (Figure 7 (b)). The results of Z ventilation layout (Figure 7 (c)) show that although the oxygen ingress patterns on the MG side are almost similar to the oxygen ingress patterns shown in Figure 7 (b) of return shaft as return system, the oxygen levels on the tailgate side are slightly higher when compared with oxygen levels shown in Figure 7 (b).

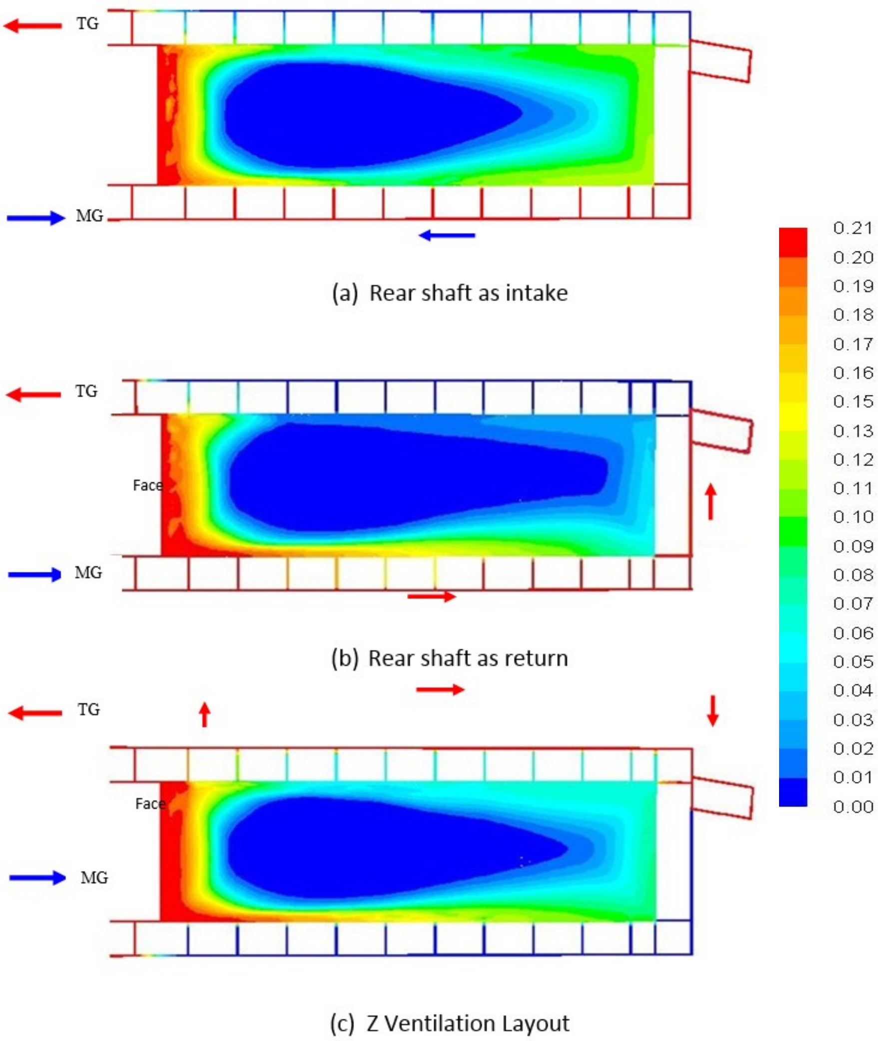

Figure 7. Oxygen distribution in the goaf with different ventilation layouts.

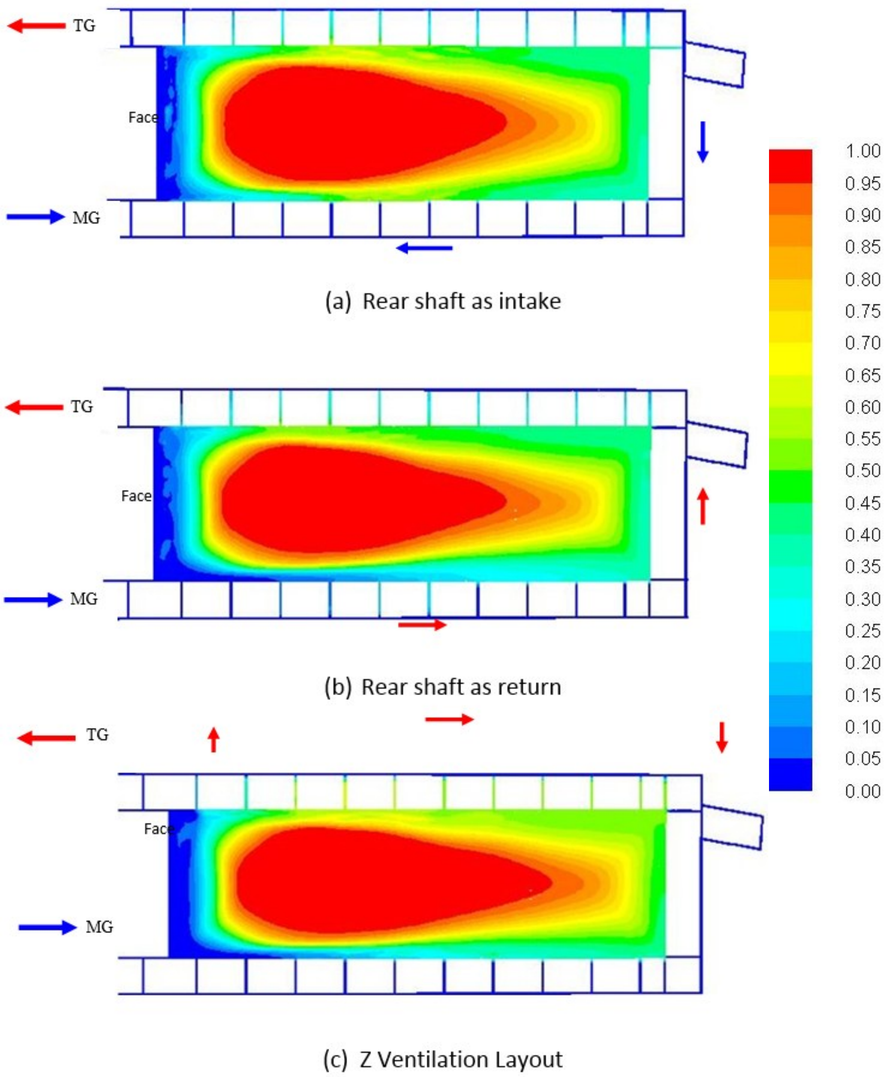

Figure 8. Methane distribution in the goaf with different ventilation layouts.

Analysis of the results presented in Figure 8 indicates that the return rear shaft ventilation system results in methane gas migration towards the back of the goaf, resulting in reduced oxygen levels on the tailgate side and near the start-up area of the panel. The return rear shaft system may also lead to a positive outbye pressure across the seals, and results in methane gas leakage from the goaf area towards the perimeter roadway. The results obtained indicate that methane gas distribution would be longer at the working seam level in the case of the return rear shaft ventilation system (Figure 8 (b)) when compared with the intake rear shaft system. The results of Z ventilation layout (Figure 8 (c)) show that the methane distribution patterns are almost similar to the methane distribution with return shaft as return system. It is to be noted here that these simulations were carried out without goaf gas drainage and without inertization in order to obtain a fundamental understanding of the effects of various individual parameters.

5.3. Effect of regulator in MG on inbye side of LW face

Regulators are being used on the MG side of the longwall panels at few of the Australian coal mines with very low propensity to sponcom to manage goaf gas concentration levels and gas drainage. The concept was to install a regulator on MG of the panel behind the face line to create a negative pressure in the perimeter roadway in order to create a positive outbye pressure across the seals to minimize air leakage into the goaf, and to drain methane gas from the seal just inbye of the regulator [20]. The CFD modelling simulation was carried out to investigate the effect of the concept of MG regulator on the goaf gas flow patterns and distribution. The results of the modelling simulations showing oxygen distribution in the goaf with and without MG regulator are presented in Figure 9. In both simulations, the goaf gas emission rate was specified at 4,000 l/s and return rear shaft ventilation system for comparison purposes. Analysis of the results obtained shows that installation of MG regulator results in a negative pressure in the perimeter roadway and a positive outbye pressure across the seals as per the objective of the regulator concept.

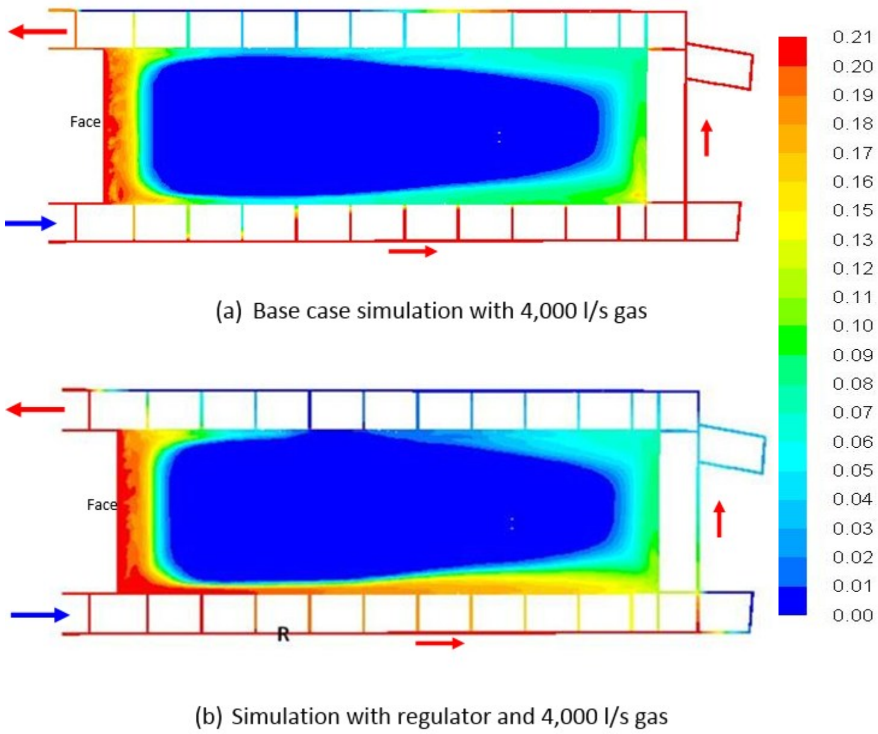

Figure 9. Oxygen distribution in the goaf with and without MG regulator (rear shaft as return).

However, the results also showed that installation of the MG regulator also led to increased air/oxygen ingress from the face area into the goaf on the MG side, resulting in very high oxygen levels of over 14% even at 800 m behind the face. The results indicate that although installation of the MG regulator might lead to a reduced oxygen leakage into the goaf through seals due to a negative pressure in perimeter roadway, it can also lead to an increased oxygen ingress from the face area into the goaf. Therefore, installation of the MG regulator requires a delicate balancing act to avoid oxygen ingress from the face area into the goaf. In addition, sometimes practical issues such as not shifting the regulator regularly with face retreat might result in very high oxygen ingress into the goaf area, which would increase the heating/fires risk significantly in sponcom prone mines.

5.4. Effect of seals leakage

Air leakage through seals depends on designs and standards of construction of seals in addition to the geotechnical structural issues and ventilation pressure distribution around the longwall panels. It is also known that minute fractures can also develop in the seals and the surrounding areas depending on the geological and geotechnical environment around the seals, particularly during the longwall retreat process and post-caving stress development/re-adjustment phase. In addition, air leakage characteristics of the seals can change during the longwall retreating process depending on the field mining conditions [22].

A few parametric studies were carried out to investigate the effect of seals leakage on the goaf gas flow distribution patterns. The results of the modelling simulations showing oxygen distribution in the goaf for the base-case and with the seals leakage are presented in Figures 10 and 11, respectively. In both the parametric studies presented here, permeability of the MG seal at the start-up area was increased to simulate seals leakage at around 150 l/s, and the rear shaft was used as the intake airway. In these parametric studies, the goaf gas emission rate was specified at 1,000 l/s and 4,000 l/s, respectively.

The results obtained showed that seal leakage had a substantial effect on the goaf gas flow patterns and oxygen concentration distribution in the goaf.

The oxygen concentration levels at the start-up area of the panel significantly increased up to 16-18%. Analysis of the results indicated that seals leakage not only increased the oxygen levels around the seals but also had a significant influence on the oxygen levels in the MG collapsed roadway, with oxygen levels above 12% up to 500 m distance from the leaking seal, particularly under the low gas emission scenario of around 1,000 l/s of the goaf gas emission rate.
The results presented in Figure 10 show that seal leakage has a substantial effect on the goaf gas distribution even at a higher goaf gas emission rate of around 4,000 l/s. The results also show that the oxygen concentration levels are over 12% up to 200 m distance from the leaking seal even under high goaf gas emission scenario. Analysis of the results indicated that leakage through MG seal at the start-up area of the panel would have a significant effect on the goaf gas flow patterns and oxygen distribution in the goaf under field site conditions with rear shaft as intake ventilation system.

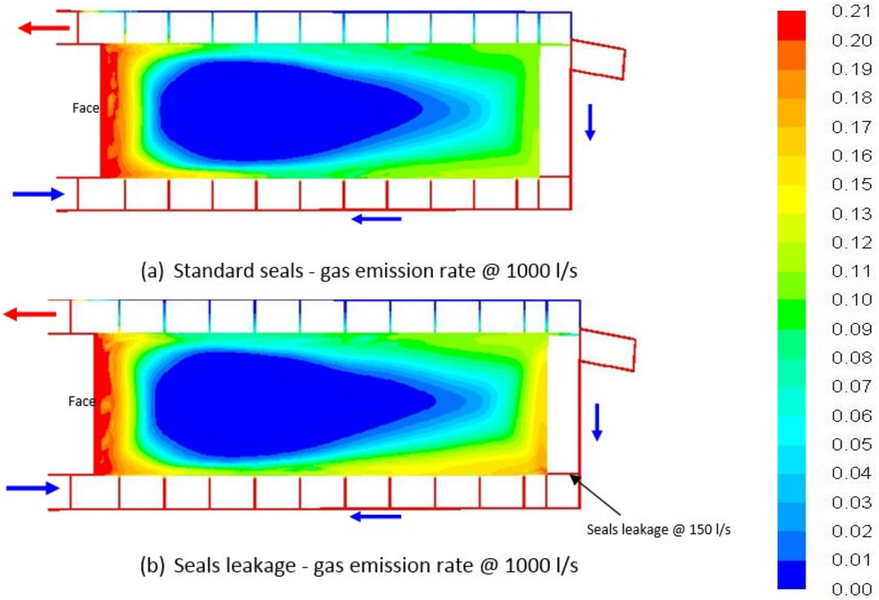

Figure 10. Oxygen distribution in the goaf with and without seals leakage–gas emission @ 1,000 l/s.

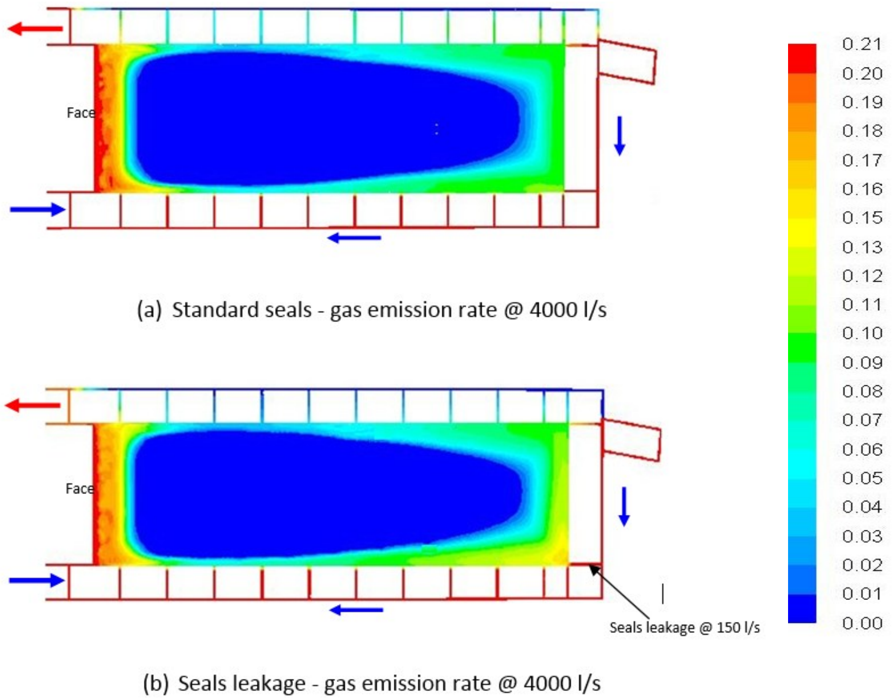

Figure 11. Oxygen distribution in the goaf with and without seals leakage–gas emission @ 4,000 l/s.

6. Conclusions

Ventilation layout: The results obtained indicated that although the general oxygen ingress distance would be higher on the MG side with return rear shaft ventilation layout, the oxygen concentration levels on the tailgate side of the panel and at the start-up area of the panel would be significantly lower under mining conditions when compared with the intake rear shaft ventilation layout. The results also indicate that return rear shaft ventilation layout/system results in methane gas migration towards the back of the goaf, resulting in reduced oxygen levels on the tailgate side and near the start-up area of the panel. The return rear shaft system may also lead to a positive outbye pressure across the seals, which minimizes air leakage into the goaf area. However, it is to be noted here that there will not be any significant difference between the effects of two ventilation layouts on the goaf gas distribution patterns when proactive inertisation is implemented in the longwall panels to minimize the sponcom risk.

Regulators on MG side: The results obtained indicate that installation of MG regulator leads to an increased air/oxygen ingress from the face area into the goaf on MG side, and results in very high oxygen concentration levels in the goaf area depending on the goaf gas emission rates. The results also indicate that although installation of MG regulator might lead to a reduced oxygen leakage into the goaf through seals due to a negative pressure in perimeter roadway, it can also lead to an increased oxygen ingress from the face area into the goaf.

Seals leakage: The results obtained indicated that seal leakage would have a substantial effect on the goaf gas flow patterns and oxygen concentration distribution in the goaf. The results also indicated that seals leakage not only increased the oxygen levels around the seals but also would have a significant influence on the oxygen levels in the MG collapsed roadway, particularly under the low goaf gas emission scenarios.

References

[1]. Saffari, A., Sereshki, F., Ataei, M. and Ghanbari, K. (2013). Applying rock engineering systems (RES) approach to evaluate and classify the coal spontaneous combustion potential in Eastern Alborz coal mines. Int. Journal of Mining & Geo-Engineering. 47 (2): 115-127.

[2]. Saffari, A., Sereshki, F., Ataei, M. and Ghanbari, K. (2017). Presenting an engineering classification system for coal spontaneous combustion potential. International Journal of Coal Science & Technology. 4 (2): 110-128.

[3]. Huang, J., Bruining, J. and Wolf, K.H. (2001). Modeling of gas flow and temperature fields in underground coal fires. Fire Safety Journal. 36 (5): 477-489.

[4]. Trevits, M.A., Yuan, L., Teacoach, K., Valoski, M.P. and Urosek, J.E. (2009). Understanding mine fires by determining the characteristics of deep-seated fires. NIOSH Document.

[5]. Proud, D., Collecutt, G. and Humphreys, D. (2015). Computational fluid dynamics modelling of coal dust explosions and suppression systems. Third Aust. Mine Vent. Conf. The Australasian Institute of Mining and Metallurgy. Sydney. Australia. pp. 309-313.

[6]. Collecutt, G., Humphreys, D. and Proud, D. (2009). CFD simulation of underground coal dust explosions and active explosion barriers. In 7th International Conference on CFD in the Minerals and Process Industries. pp. 1-6.

[7]. Ren, T.X., Plush, B. and Aziz, N. (2011). Dust controls and monitoring practices on Australian longwalls. Procedia Engineering. 26: 1417-1429.

[8]. Tanguturi, K., Balusu, R., Morla, R. and Khanal, M. (2013). Effect of buoyancy on methane gas distribution and gas control strategies at tailgate region in a gassy coal mine. In 9th International Conference on CFD in the minerals and process Industries. Melbourne. pp. 1-6.

[9]. Tanguturi, K. and Balusu, R. (2015). Fundamental understanding of goaf gas displacement in longwall goaf. Journal of Mining and Environment. 6 (2): 191-203.

[10]. Moloney, K.W., Hargreaves, D.M. and Lowndes, I.S. (1998). Computational fluid dynamics (CFD) simulations in underground auxiliary ventilated headings. In Computer applications in the minerals industries. International symposium. pp. 721-731.

[11]. Brune, J.F. and Saki, S.A. (2017). Prevention of gob ignitions and explosions in longwall mining using dynamic seals. International Journal of Mining Science and Technology. 27 (6): 999-1003.

[12]. Ren, T.X. and Edwards, J.S. (2000). Three-dimensional computational fluid dynamics modelling of methane flow through permeable strata around a longwall face. Mining technology. 109 (1): 41-48.

[13]. Yuan, L. and Smith, A.C. (2009). CFD modeling of spontaneous heating in a large-scale coal chamber. Journal of Loss Prevention in the Process Industries. 22 (4): 426-433.

[14]. Yuan, L. and Smith, A.C. (2009). Numerical Study on Spontaneous Combustion of Coal in US

Longwall Gob Areas. In Proceedings of the Ninth International Mine Ventilation Congress. pp. 10-13.

[15]. Fletcher, C.A.J., Jancar, T., Matthews, B., Guzman, M.D. and Tu, J.Y. (1995). Computational simulation for mineral processing. Proceedings APCOM XXV. pp. 361-370.

[16]. ANSYS 17.0 Documentation. ANSYS Fluent online documentation 17.0.

[17]. Launder, B.E. and Spalding, D.B. (1974). The numerical computation of turbulent flows. Computer Methods in Applied Mechanics and Engineering. 3 (2): 269-289.

[18]. Versteeg, H.K. and Malalasekera, W. (2007). An introduction to computational fluid dynamics: the finite volume method. Pearson Education.

[19]. Patankar, S.V. (1980). Numerical heat transfer and fluid flow. Hemisphere Publication Corporation. Washington.

[20]. Gillies, A.D.S., Wu, H.W., Mayes, T.I. and Halim, A. (2002). Measurement of airflow through regulators and real time integrated monitoring. In Proceedings Northern American Ninth US Mine Ventilation Symposium. pp. 301-308.

[21]. Gillies, S. and Wu, H. W. (2013). Australian longwall panel ventilation practices. 13th Coal Operators' Conference. University of Wollongong. The Australasian Institute of Mining and Metallurgy & Mine Managers Association of Australia. pp. 176-183.

[22]. Schatzel, S.J., Krog, R.B., Mazzella, A., Hollerich, C. and Rubinstein, E. (2016). A study of leakage rates through mine seals in underground coal mines. International journal of mining, reclamation and environment. 30 (2): 165-179.

شبیه‌سازی دینامیک سیالات محاسباتی برای بررسی پارامترهای تأثیرگذار در توزیع گاز در ناحیه تخریب شده

K.M. Tanguturi and R.S. Balusu

Energy Flagship, CSIRO, Pullenvale, Kenmore, Australia

ارسال ۲۰۱۷/۷/۳، پذیرش ۲۰۱۸/۲/۱۳

* نویسنده مسئول مکاتبات: krishna.tanguturi@csiro.au

چکیده:

برای درک اساسی در مورد الگوهای جریان گاز در ناحیه تخریب شده در معادن جبهه کار طولانی لازم است تا الگوهای جریان گاز در ناحیه تخریب در معادن جبهه کار طولانی مشخص شود تا از این طریق راهکارهای بهینه‌ی گاز کشی و مدیریت خودسوزی در این ناحیه به دست آید. به منظور گاز کشی از ناحیه تخریب شده باید بهترین طرح تهویه برای یک معدن جبهه کار طولانی اختصاص یابد تا خطر خودسوزی در این ناحیه به حداقل مقدار ممکن کاهش یابد. علاوه بر این، در پهنه‌های جبهه کار طولانی تنظیم‌کننده‌های جریان هوا در راهروهای اصلی نصب می‌شوند تا انتقال گاز در اطراف این راهروها کنترل شود، زیرا معدن کاران اغلب با مشکلات نشت گاز مواجهه می‌شوند. مطالعات پارامتری گسترده‌ای برای بررسی تأثیر طرح تهویه، تنظیم‌کننده‌ها، پوشش‌های هوابند برای جلوگیری از نشت در توزیع گاز در ناحیه تخریب شده با استفاده از روش‌های دینامیک سیالات محاسباتی (CFD) انجام شده است که در این پژوهش نتایج و جزئیات شبیه‌سازی‌های مختلف CFD ارائه شده است.

کلمات کلیدی: CFD، طرح تهویه، ناحیه تخریب شده، چاه برگشت، هوابند، تنظیم‌کننده‌ها.